

Detection of wave aberrations in the human eye using a retinoscopy-like technique

María Teresa Caballero ^a, Walter D. Furlan ^{b,*}, Amparo Pons ^b, Genaro Saavedra ^b,
Manuel Martínez-Corral ^b

^a *Departamento de Óptica, Universidad de Alicante, 03080 Alicante, Spain*

^b *Departamento de Óptica, Universitat de València, clo Dr. Moliner 50, E-46100 Burjassot, Spain*

Received 13 June 2005; accepted 11 November 2005

Abstract

The influence of optical aberrations on the retinoscopic reflex is theoretically analyzed from a geometrical point of view. The relationship between the wave aberrations to the ray aberrations is applied to explain the appearance of the retinoscopic patterns for different types of ocular aberrations. Several schematic models of the human eye are tested numerically, showing that a careful retinoscopic examination can detect the usual eye aberrations.

© 2005 Elsevier B.V. All rights reserved.

1. Introduction

The design of techniques for the objective measurement of refraction in the human eye has aimed many research efforts in the past and still attracts the interest of scientists [1,2]. Retinoscopy is a classical and certainly the most common technique to perform this measurement [3]. A standard streak retinoscope has a light source consisting of a straight-filament bulb that is located in the handle of the instrument. The light proceeding from the source is reflected in a beam splitter towards the patient's eye forming an image of the glowing filament at the retina. This stripe-like spot of light acts as a secondary source of light, playing a role equivalent to that played by the illumination slit in the classical Foucault knife-edge test [4]. The observer (the retinoscopist) views through the retinoscope sight-hole aperture the light that is diffusely reflected by the retina and emerges from the pupil of the patient's eye. The observed pattern at the patient's pupil is called 'the reflex'. Tilting the retinoscope, about an axis perpendicular to the optical axis, causes the spot to shift its eccentricity

from the sight-hole and, depending mainly on the eye's ametropia, to change the appearance of the reflex. For an aberration-free eye, when the retina is made conjugate with the retinoscope pupil plane (by means of the proper ophthalmic trial lens), and the retinoscope is tilted, the pupil of the eye suddenly switches from bright to dark without any apparent motion. This situation is known as the 'neutralization' of the reflex, and directly provides the refractive state of the eye.

In practice, the aberrations of the eye are considered as a handicap because they make the point of neutralization rather imprecise. In fact, as happens in any *null test*, transverse aberrations modify the boundary of the dark and bright regions of the retinoscopic reflex. This fact was recognized by several authors in early attempts to measure the degree of aberration of the human eye by measuring refraction isolating different zones of the pupil [5,6]. From a theoretical point of view, several analyses of retinoscopy can be found in the literature (see for example [3]). Most of them only consider refractive errors and the global effect of aberrations on this technique was not considered until the work of Roorda and Bobier [7]. They use a geometrical-optics approach to analyze the retinoscopic reflex for a reduced eye model with aberrations. By representing in

* Corresponding author. Fax: +34 963 864 715.

E-mail address: walter.furlan@uv.es (W.D. Furlan).

a contour plot the succession of reflexes across the pupil for each position of the retinoscope, they show that retinoscopy can be considered a measure of the transverse ray aberration of the eye. However, to our knowledge, the relationship between these geometric aberrations and the wave aberrations of the eye has not been explicitly asserted in the literature.

Nowadays the measurement of wave aberrations of the eye has become a standard practice in several ophthalmologic routines [8]. The influence of aberrations on the ocular refractive state is of crucial importance, especially when refractive surgery is considered [9]. In this context, it is necessary the classical techniques of ocular inspection to be adapted to monitor ocular aberrations, becoming in this way alternative diagnostic tools. In this paper we propose a theory that quantitatively relates the observed patterns in retinoscopy with the wave aberration of the eye. We use this theoretical result to simulate the retinoscopic-like examination of different model eyes. The use of schematic eye models allows the evaluation of the performance of the retinoscope as a tool for detecting aberrations in real eyes.

2. Wave and ray aberrations in retinoscopy

The geometrical theory of image formation can be used to show the potential ability of retinoscopy to detect eye aberrations. For simplicity, let us consider the geometry of a retinoscopic measurement of an aberrated myopic eye with its far point located at a distance R^{-1} from it (R being the eye's ametropia, see Fig. 1). The retinoscopist tilts the retinoscope changing the illumination beam eccentricity and driving the beam (not shown in Fig. 1) across the pupil of the examined eye (monochromatic illumination is assumed [10]). This movement causes a displacement of the secondary source at the retina with respect to the fixed sight-hole aperture. At every position, in a second pass through the eye, rays emerging from different points at the retina reach the pupil of the retinoscope, which blocks part of the beam coming from the patient's eye. Thus, to analyze a complete scope along one of the eye's meridians different optical axes must be defined, one for each source position. In order to simplify the analysis we use an alternative frame of reference (as in [7]) in which the sight-hole

aperture moves with respect to the fixed source. Although this approach is not fully equivalent to conventional retinoscopy, it is even simpler to implement experimentally. In this context the analysis can be further simplified if the sight-hole is supposed to have one straight border that behaves like a knife-edge traveling transversally to the optical axis at the sight-hole aperture plane.

Returning to Fig. 1, a real ray emerging from a retinal point, passing through the pupil at the point (x, y) crosses the reference Gaussian image plane (which we define at the axial position of the retinoscope) at the point (x_1, y_1) . These coordinates are the difference between the aberrated and non-aberrated images of the point object at the retina, and give the components of the ray aberration. Assuming that the light scattered back from the retina in the foveal region has an isotropic intensity distribution, it can be shown that ray aberration and the wave aberration, $W(x, y)$ are approximately related [11] by

$$(x_1, y_1) = \frac{1}{E} \left(\frac{\partial W(x, y)}{\partial x}, \frac{\partial W(x, y)}{\partial y} \right), \quad (1)$$

where E^{-1} is the so-called *working distance* (see Fig. 1).

According to our assumptions, during a scanning along the x axis, the moving border of the retinoscope pupil can be thought as a spatial filter whose transmittance can be expressed as

$$T(x_1, y_1) = \begin{cases} 1 & \text{if } \left(\frac{\partial W(x, y)}{\partial x} \right) \leq dE, \\ 0 & \text{if } \left(\frac{\partial W(x, y)}{\partial x} \right) > dE, \end{cases} \quad (2)$$

where d is the variable distance between the border of sight-hole of the retinoscope and the optical axis (see Fig. 1). In each position d_i the boundary between the bright and dark regions varies according to Eq. (2). This means that, if the aberrations of the eye are known, the observed patterns in the retinoscopic examination can be predicted by this equation. Additionally, Eq. (2) allows computing these patterns at any axial position and for any refractive state of the eye, provided that the defocus coefficient of the aberration wave function, W_{20} , can be expressed in terms of R and E as [12]

$$W_{20} = \frac{E - R}{2}. \quad (3)$$

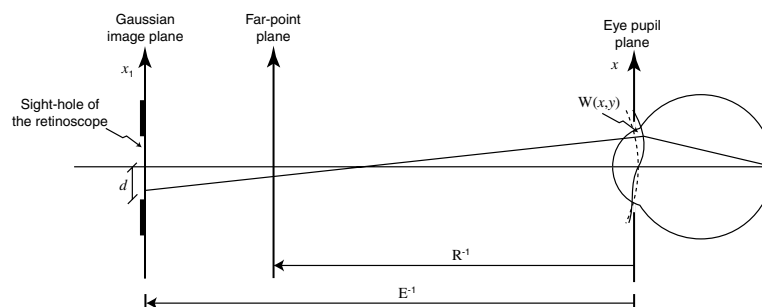


Fig. 1. Aberrated myopic eye examined with a retinoscope at a distance E^{-1} (see the text for details).

Clearly, neutralization is obtained when $E = R$. For practical purposes optical aberrations can be detected better when this particular situation is achieved and, as we already mentioned, this is always possible by interposing the proper ophthalmic trial lens in front of the eye or even better by means of a Badal optometer. The influence of the intrinsic aberrations of the trial lens or Badal optometer can be eliminated by a calibration process with an artificial eye.

The aberrations of the eye also affect the first passage of the light through the eye causing an extended spot of secondary sources. In our approach this spot is considered sufficiently small such as the aberrations be the same for all points on the retinal image. Then, the retinoscopic pat-

tern will be slightly blurred by the superposition of the contributions of each point. In practice this is a limitation of the technique that can be minimized by using a small pupil size in the illumination beam, in a way that the eye can be considered almost as a diffraction limited system for the incoming light.

As an example, we have computed retinoscopic patterns for a myopic spherical-aberrated eye observed in an axial position between the marginal and the paraxial foci. Using a point-like secondary source at the retina the appearance of a retinoscopic scoping along the horizontal meridian (i.e., the sequence of images of the eye pupil obtained when the knife edge travels along the x coordinate) for different values of d is shown in Fig. 2(a). The succession of binarized

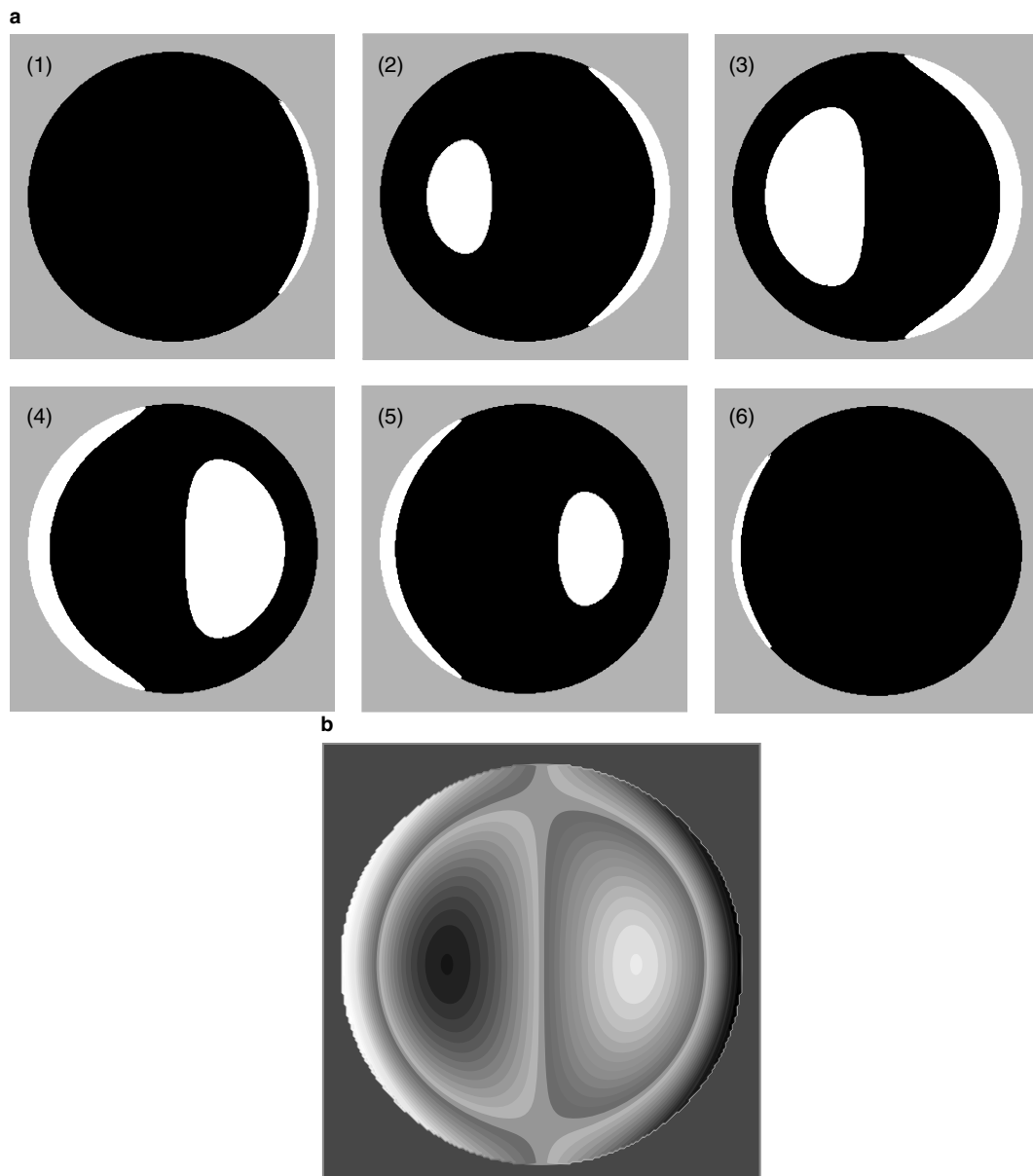


Fig. 2. (a) Set of binarized sequential images of the wave front derivatives observed in a screening of the horizontal meridian; (b) Contour map obtained as a superposition of the images in part (a).

intensity profiles at each source position can be viewed in a single figure if a different gray level is assigned to each one and all of them are superimposed as shown in Fig. 2(b). In this way each gray level represents one frame of the hypothetical movie that could be registered behind of the retinoscope. This contour map of the succession of reflexes is especially instructive since it represents a map of the first order derivative of the wavefront aberration in the direction of the sweeping of the retinoscope. A very interesting potential application of this result is that this map of derivatives, which can be obtained experimentally in two orthogonal meridians, can be integrated numerically to obtain the wave aberration of the eye.

3. Results for different eye models with aberrations

In order to check the performance of our proposal, several modern schematic eyes were tested: Lotmar [13], Kooijmann [14], Navarro [15], and Liou and Brennan [16]. The constructional data in most of these models fit anatomical data by incorporating aspherical surfaces to the classical Le Grand full theoretical eye. Particularly, a model of a gradient index lens was incorporated in [15]. The aberration values considered are listed in Table 1. These values correspond to a pupil radius of 4 mm, and fit those reported by Smith and Atchison [17], being the values for the model of Liou and Brennan the closest to the mean of real eyes.

For the case of rotationally symmetrical aberrations we first considered spherical aberration and defocus. In this case the wave aberration function is

Table 1

Wave aberration coefficients for the different schematic eyes in this study

	Lotmar	Kooijman	Navarro	Liou and Brennan
Spherical aberration (W_{40})	20.314	15.767	13.863	7.375
Coma (W_{31})	7.111	6.283	7.058	1.675

These values correspond to pupil radii of 4 mm and are given in units of wavelengths ($\lambda = 589$ nm).

$$W(x, y) = \frac{(E - R)}{2}(x^2 + y^2) + W_{40}(x^2 + y^2)^2. \quad (4)$$

By introducing Eq. (4) into Eq. (2) and solving this last equation for different values of d and E , a map of the first derivative along the x direction of the aberrated wavefront for the different models is obtained. Fig. 3 shows the results for the calculated retinoscopic reflexes at two different planes for the spherical aberration values in Table 1. In this figure the contour plots are displayed in grey levels. These results are especially instructive since spherical aberration is the dominant one when the eye is well aligned with the retinoscope. Typical reflexes can be observed in all models.

As an example of asymmetric aberrations we investigated the effects of primary coma. In this case, when no other aberrations are present, the wave aberration is expressed as

$$W(x, y) = W_{31}\eta x(x^2 + y^2), \quad (5)$$

where η is the off-axis position of the object along the x coordinate. In Fig. 4 the net effect of this aberration observed at the paraxial focal plane image is shown for

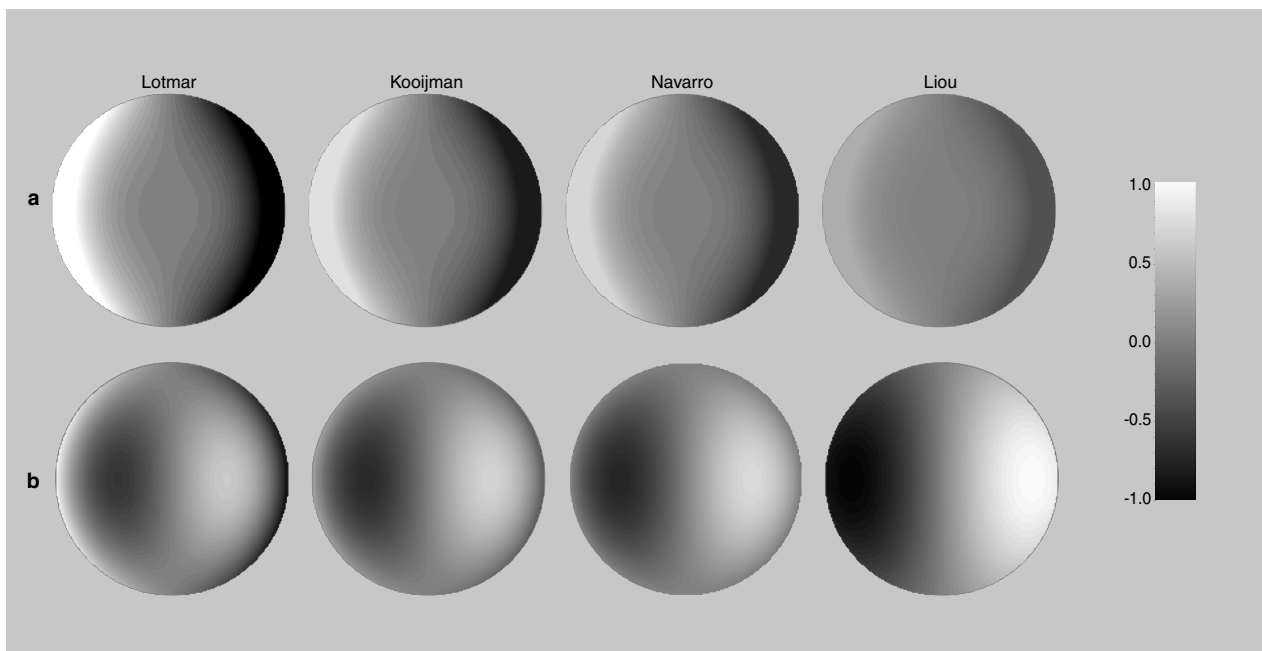


Fig. 3. Retinoscopic maps showing partial derivatives of spherically aberrated eyes (see the values in Table 1). (a) No defocus ($E = R = -2D$). (b) $E = -4D$, $R = -2D$.

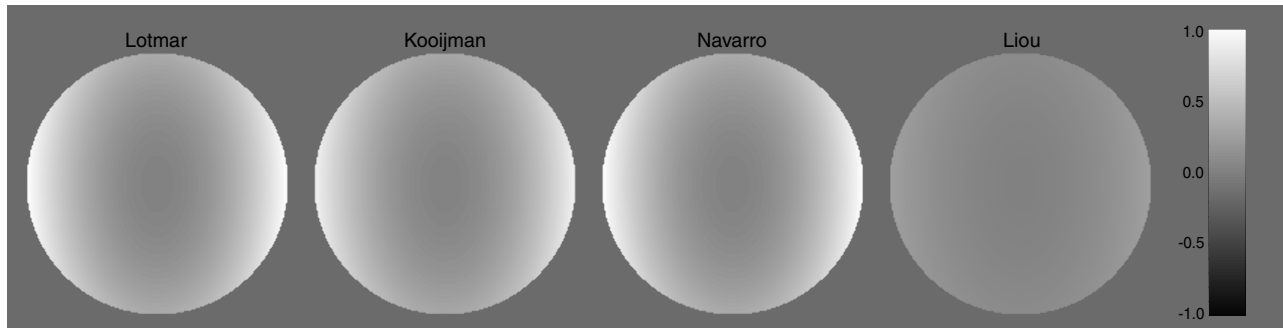


Fig. 4. Retinoscopic maps showing partial derivatives of the aberration wavefront for the eye models in Table 1, with coma ($\eta = 2$ mm).

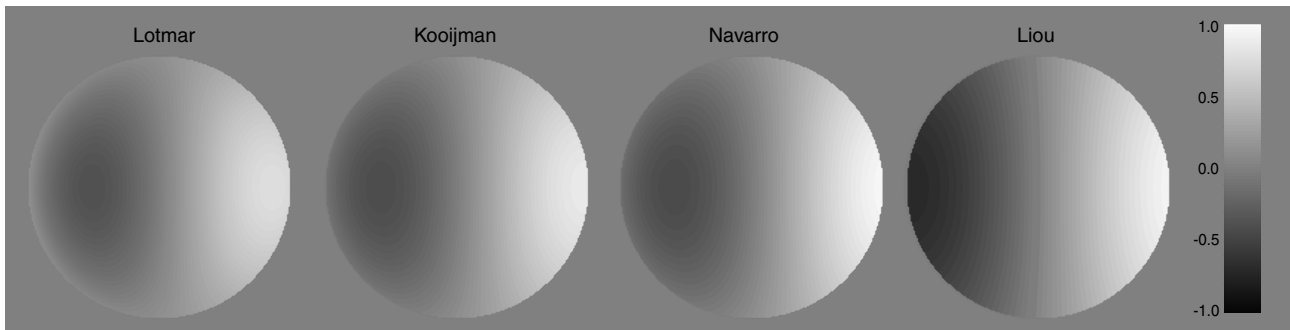


Fig. 5. Retinoscopic maps showing partial derivatives of the aberration wavefront for the eye models in Table 1 with coma ($\eta = 2$ mm), spherical aberration and defocus ($E = -4D$, $R = -2D$).

the different models of the eye. Finally the combined effect of spherical aberration, coma and defocus is shown in Fig. 5.

4. Conclusions

We have presented a theoretical analysis of retinoscopy taking into account the aberrations of the eye. Specifically, the analytical expression we found that relates the ray aberration to the wave aberration allows us to show that the succession of the retinoscopic reflexes can be computed as the partial derivatives of the wavefront along the direction of the scanning. Numerical simulations of retinoscopy were performed using schematic eye models suffering from different amount of aberrations. In addition to demonstrate that retinoscopy can be used for the detection of aberrations, it was shown that the succession of the retinoscopic reflexes during the scoping of a single meridian results as a map of the partial derivative of the wavefront along this direction. This fact opens the possibility of measuring the aberrated wave-front from two orthogonal retinoscopic measurements. Compared with the classical Hartmann–Shack this new method is more versatile since it presents almost continuous sampling and adjustable dynamic range. Thus, this paper not only brings new lights on the potential applications of retinoscopy, but also can be considered as the first step in the design of a new versatile objective eye aberrometer, which will be reported in a forthcoming paper.

Acknowledgements

This research has been supported by the following Grants: DPI 2003-04698 (Plan Nacional I+D+I Ministerio de Ciencia y Tecnología, Spain), *grupos* 03/227 (Generalitat Valenciana, Spain), and GV04B-186 (Generalitat Valenciana, Spain).

References

- [1] Y. Chen, B. Tan, J.W.L. Lewis, *Opt. Express* 11 (2003) 1628.
- [2] D.G. Hunter, K.J. Nusz, N.K. Gandhi, I.H. Quraishi, B. Gramatikov, D.L. Guyton, *J. Biomed. Opt.* 9 (2004) 1103.
- [3] A. Bennett, R. Rabbets, *Clinical Visual Optics*, Butterworth-Heinemann, Oxford, 1989 (Chapter 17).
- [4] A. Sagan, S. Nowicki, M. Kowalczyk, T. Szoplik, *Appl. Opt.* 42 (2003) 5816.
- [5] G.H. Stine, *Am. J. Ophthalmol.* 13 (1930) 101.
- [6] T.C. Jenkins, *Br. J. Physiol. Opt.* 20 (1963) 59.
- [7] A. Roorda, W.R. Bobier, *J. Opt. Soc. Am. A* 13 (1996) 3.
- [8] L.N. Thibos, X. Hong, *Optom. Vis. Sci.* 76 (1999) 8171.
- [9] S. Marcos, *Opt. Photon. News* 26 (2001) 22.
- [10] C.W. Bobier, J.G. Sivak, *Am. J. Optom. Physiol. Opt.* 57 (1980) 106.
- [11] M. Born, E. Wolf, *Principles of Optics*, Cambridge University Press, Cambridge, 1999 (Chapter 5).
- [12] V. Mahajan, *Aberration Theory Made Simple*, SPIE Optical Engineering Press, Bellingham, Washington, 1991 (Chapter 1).
- [13] W. Lotmar, *J. Opt. Soc. Am.* 61 (1971) 1522.
- [14] A. Kooijman, *J. Opt. Soc. Am.* 73 (1983) 1544.
- [15] R. Navarro, J. Santamaría, J. Bescós, *J. Opt. Soc. Am. A* 2 (1985) 1273.
- [16] H. Liou, N. Brennan, *J. Opt. Soc. Am. A* 14 (1997) 1684.
- [17] D. Atchison, G. Smith, *Optics of the Human Eye*, Butterworth-Heinemann, Oxford, 2000, A3.